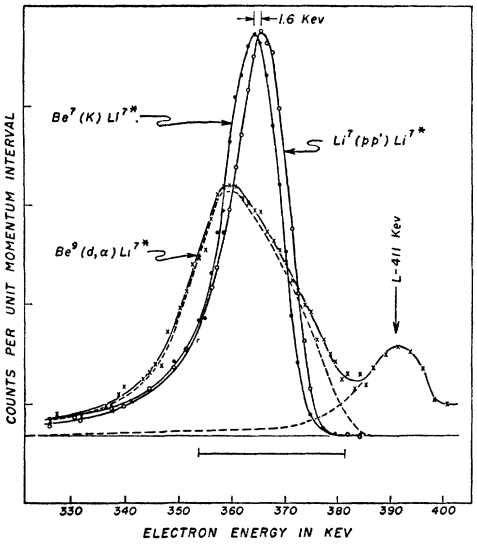

FIG. 2. K photoelectrons ejected from 7.0 mg/cm² of thorium by the 477 kev gamma-ray line from Li^7. The horizontal line just below the curves represents the maximum Doppler effect in the $Be^9(d, \alpha)Li^{7*}$ reaction.

angular distribution of the photoelectrons and on the target geometry; a rough estimate of these effects yields a value of about 0.8. Scattering in the converter will tend to lower the apparent shift and broaden the line. In the center of mass system, the motion of the Li^{7*} will tend to broaden the line, without shifting the peak, the amount of broadening being

$$\Delta_2 = 2E_\gamma(V_{cm}(\mathrm{Li}^7)/c).$$

If the gamma-ray emission is isotropic and is not correlated with the Li^7 direction, the observed peak should be rectangular with the sides rounded off by the effect of finite resolution; translation to the laboratory system shifts the center of the rectangle toward higher energy by an amount Δ_1. It is quite clear from Fig. 2 that the observed curve deviates markedly from this simple shape.

Three possible explanations for the deviation suggest themselves: First, the Li^7 nuclei may not be isotropically emitted with respect to the bombarding beam or there may be some correlation between the direction of motion of a Li^7 nucleus and the gamma-ray it emits. Second, additional gamma-rays near 477 kev may be present, although this offers no convincing explanation of the shape observed. Third, some of the Li^{7*} nuclei may be stopped before they radiate. Since the gamma-ray transition involved is usually taken as $^2P_{1/2}-{}^2P_{3/2}$, magnetic dipole radiation is the most probable allowed radiation, and the half-life of the state should be of the order of 10^{-13} sec. The range of a 4 Mev Li^7 nucleus in beryllium is around 6×10^{-4} cm and the mean velocity is 0.5×10^9 cm/sec. The Li^7 nuclei will therefore be stopped in a time comparable with the half-life of the excited state, except when they can escape from the target in the backwards direction. Since the yield of the $Be^9(d, \alpha)Li^7$ reaction is rising steeply at this energy, most of the Li^7 will be made in the first thin ($\sim10^{-4}$ cm) layer of the target. The stopping would result in a deficiency of nuclei emitting with the maximum forward velocity, while the number contributing to the "red shift" region would be much less affected.

The above considerations apply also to the shift and broadening of the peak obtained from the $Li^7(p, p')Li^{7*}$ reaction, although, in this case, the lower density of the Li^7 metal and its lower stopping power for the Li^{7*} nuclei result in a somewhat longer stopping time. The fact that a definite shift is observed indicates that the lifetime of Li^{7*} cannot be long compared to 10^{-12} sec.

We are much indebted to Professor R. F. Christy for assistance in the analysis of the problem. This work was assisted by the Joint Program of the Office of Naval Research and the Atomic Energy Commission.

[1] T. Lauritsen, W. A. Fowler, C. C. Lauritsen, and V. K. Rasmussen, Phys. Rev. **73**, 636 (1948).
[2] T. Lauritsen, C. B. Dougherty, and V. K. Rasmussen, Bull. Am. Phys. Soc. **23**, 5, 16 (1948).
[3] We are greatly indebted to Professor R. W. Richardson of the University of California at Los Angeles for making the Be^7 for us and to Professor D. M. Yost of the California Institute of Technology for making the chemical separations involved.
[4] Effects of order v^2/c^2 have been neglected.

Isotopic Weights of Medium Elements

K. OGATA
Department of Physics, Faculty of Science, Osaka University, Osaka, Japan
September 20, 1948

ISOTOPIC weights of all the isotopes of Cr, Fe, Zn, and Br were determined with a Bainbridge-Jordan type mass-spectrograph. Glow discharge in a cylindrical tube was used as the ion source. A brief account of the result is as follows:

1. *Chromium.* Discharge through the vapor mixture of n-CrH_{16} and chromyl chloride (CrO_2Cl_2) produced doublets, whose mass differences were as follows:

Doublets	Number of doublets measured	Mass differences ($\times10^{-4}$ M.U.)
$C^{12}{}_4H^1{}_{12}-Cr^{50}$	6	673.2±3.7
$C^{12}{}_4H^1{}_{14}-Cr^{52}$	17	920.3±4.2
$C^{12}{}_4H^1{}_{15}-Cr^{53}$	13	1008.7±4.1
$C^{12}{}_4H^1{}_{16}-Cr^{54}$	7	1100.0±4.6

2. *Iron.* Iron carbonile (Fe(CO)) was prepared as the volatile iron. Discharge was passed through the mixture of its vapor and normal heptane vapor. The measured doublets and their mass differences were as follows:

Doublets	Number of doublets measured	Mass differences ($\times10^{-4}$ M.U.)
$C^{12}{}_4H^1{}_{16}-Fe^{54}$	10	1065.3±4.7
$C^{12}{}_4H^1{}_{18}-Fe^{56}$	23	1271.3±2.3
$C^{12}{}_4H^1{}_{19}-Fe^{57}$	15	1338.1±5.0
$C^{12}{}_4H^1{}_{10}-Fe^{58}$	4	1458.8±4.7

3. *Zinc.* A small electric crucible which contained small pieces of Zn metal was introduced in the discharge tube. N-heptane vapor sustained the discharge, while the zinc was vaporized by electric heating. Doublets and mass differences obtained were as follows:

Doublets	Number of doublets measured	Mass differences ($\times 10^{-4}$ M.U.)
$C^{12}_5H^1_{14}-Zn^{64}$	13	982.3±6.4
$C^{12}_5H^1_{16}-Zn^{66}$	17	1213.8±3.9
$C^{12}_6H^1_7-Zn^{67}$	8	1280.1±6.3
$C^{12}_6H^1_8-Zn^{68}$	8	1355.5±6.3
$C^{12}_6H^1_{10}-Zn^{70}$	3	1346.0±16

4. *Bromine.* Discharge was operated through the mixture of normal heptane vapor and sublimated vapor of titanium tetrabromide crystals. Since doublets could not be obtained in this case, dispersion curves were drawn by the least square method with five hydrocarbon lines, $C^{12}_3H^1_2$, $C^{12}_3H^1_3$, $C^{12}_3H^1_4$, $C^{12}_3H^1_5$, and $C^{12}_3H^1_6$, which covered the doubly ionized region of Br. From these dispersion curves and the mass $H^1=1.0081$, the following mass differences were obtained:

Mass differences	Number measured
$\frac{1}{3}Br^{79}-C^{12}_3H^1_3=0.43618\pm2.3\times10^{-4}$	11
$\frac{1}{3}Br^{81}-C^{12}_3H^1_4=0.42700\pm1.6\times10^{-4}$	11

From these above results of the mass differences and the value $H^1=1.008131\pm0.033\times10^{-4}$, $C^{12}=12.003871\pm0.33\times10^{-4}$,[1] the isotopic weights of all these isotopes were calculated. The isotopic weights, the packing fractions, and the binding energies which were calculated from the mass of hydrogen (1.008131) and neutron (1.008945) are summarized in Table I. In the last column are given theoretical binding energies, calculated from Nakabayashi's formula of the binding energy,[2]

$$E=-15.2A+20(N-Z)^2/A+14.6A^{\frac{2}{3}}+0.62Z^2A^{-\frac{1}{3}}(10^{-3}\text{ M.U.})$$

here, A is mass number, Z is number of protons, and N is number of neutrons.

The packing fraction curves were drawn in this region by using these results and the values of Ti[3] and Ni[4] reported in our previous paper.

It is seen from these curves (Fig. 1) that the packing fraction of the isotopes of the same elements differ considerably from each other. It is worth noticing especially that in the four pairs of isobars, $Ti^{50}-Cr^{50}$, $Cr^{54}-Fe^{54}$, $Fe^{58}-Ni^{58}$, and $Ni^{64}-Zn^{64}$, the packing fraction of larger atomic number elements is always larger algebraically than that of small atomic number elements. The dotted line in this figure shows the general tendency of the packing fraction curves in this region. It is seen from these curves that Dempster's packing fractions[5] in this region are slightly large, and that the minimum of our packing fraction curve is located about Cr or Fe, though in Dempster's curve it is located about Ti.

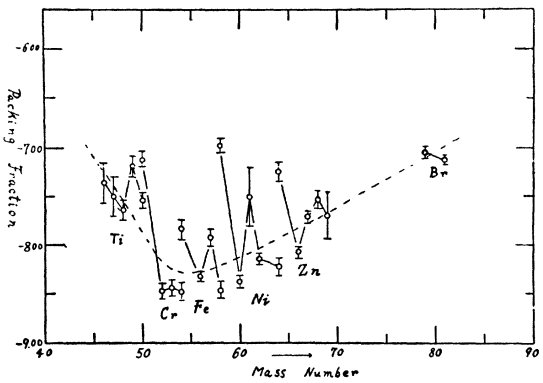

FIG. 1. Packing fraction curve in the region Ti to Br.

TABLE I.

Element	Z	A	Isotopic weight	Packing fraction	Binding energy (10^{-3} M.U.) Exp.	Theor.
Cr	2	50	49.96443± 3.9×10⁻⁴	−7.11±0.08	463.3	463
		52	51.95598± 4.4×10⁻⁴	−8.47±0.08	489.6	485
		53	52.95527± 4.4×10⁻⁴	−8.44±0.08	499.3	495
		54	53.95427± 4.8×10⁻⁴	−8.47±0.09	509.2	504
Fe	26	54	53.95774± 4.8×10⁻⁴	−7.83±0.09	504.1	500
		56	55.95340± 2.7×10⁻⁴	−8.32±0.05	526.4	522
		57	56.95485± 5.2×10⁻⁴	−7.92±0.09	533.9	532
		58	57.95091± 4.9×10⁻⁴	−8.46±0.09	546.7	542
Zn	30	64	63.95365± 6.6×10⁻⁴	−7.24±0.10	594.4	594
		66	65.94676± 4.2×10⁻⁴	−8.07±0.06	619.2	616
		67	66.94826± 3.8×10⁻⁴	−7.71±0.06	626.6	625
		68	67.94885± 6.5×10⁻⁴	−7.53±0.09	635.0	635
		70	69.9461 ±17 ×10⁻⁴	−7.69±0.24	655.4	652
Br	35	79	78.94438± 5.0×10⁻⁴	−7.04±0.06	733.8	735
		81	80.94228± 3.8×10⁻⁴	−7.12±0.05	753.8	752

[1] K. Ogata, Proc. Phys.-Math. Soc. (Japan) **22**, 486 (1940).
[2] Private communication.
[3] T. Okuda and K. Ogata, Proc. Phys.-Math. Soc. (Japan) **25**, 374 (1943).
[4] T. Okuda, K. Ogata, H. Kuroda, S. Shindo, and S. Shima, Phys. Rev. **59**, 104 (1941).
[5] A. J. Dempster, Phys. Rev. **53**, 64 (1938).

Cloud-Chamber Evidence of a Meson-Nucleus Interaction*

G. E. VALLEY, C. P. LEAVITT, AND J. A. VITALE

Physics Department and Laboratory for Nuclear Science and Engineering, Massachusetts Institute of Technology, Cambridge, Massachusetts

November 12, 1948

IN September 1948 we successfully operated a cloud chamber filled with argon to a pressure of 105 atmospheres (at 15°C) in a magnetic field of 8800 gauss, and at an altitude of 12,730 feet above sea level (by Summit Lake on Mt. Evans in Colorado). Stereoscopic pictures